技術論文

Fuel Film Behavior Analysis Using Simulated Intake Port

Minoru Iida, Keiichi Yoshikawa, Hiroshi Tanaka, G. Wang, C. Arcoumanis

Reprinted with permission (c) 2009 SAE Japan and SAE International.

要旨

モータサイクルにとって、エンジンの過渡挙動は非常に重要な要素である。ポート内の燃料噴射により形成される燃料液膜は、過渡挙動はもちろん、エンジンのほかの性能：出力・排ガス・燃費にも大きな影響を及ぼしている。燃料液膜に関して実機エンジンで起こる現象は、噴霧の微粒化・蒸発・壁面衝突・付着・再微粒化、液膜からの蒸発・再微粒化、液膜の移動が同時かつ非定常的に進行するため、非常に複雑である。そこで今回の研究では、これらの現象を分離して捉えるため、ポート模擬管を用い、定常空気流中での噴霧液膜挙動を分析した。液膜厚さはレーザ誘起蛍光法にて計測し、液膜の発達は高速度ビデオにより捕らえた。当論文では、燃料性状・噴射量・噴射間隔・空気流速・背圧の影響を定量化した。その結果、イソオクタンとガソリンの挙動は異なること、噴射量増大は必ずしも液膜量増大に結びつかず液膜拡散効果があること、低背圧は液膜の拡散を阻害することなどがわかった。

Abstract

Transient behavior of the engine is one of the most crucial factors among the features of a motorcycle. Characterization of the fuel film with port fuel injection (PFI) is necessary to enhance this feature, while maintaining others such as high output, low emissions and good fuel consumption. In order to resolve the complicated phenomena in real engine conditions into simple physical issues, a simulated intake port was used in our research with Laser Induced Fluorescence (LIF) technique to enable accurate measurement of the fuel film thickness, complemented by visualization of the film development and spray behavior using high-speed video imaging. Useful results have been obtained from the parametric studies with various sets of conditions, such as injection quantity, air velocity and port backpressure.

1 INTRODUCTION

Port fuel injection (PFI) system widely used for majority of the gasoline-fuelled automotive engines. Combining this with other systems, such as catalytic converter and engine control system, automotive engines perform very clean and efficient without sacrificing output. This kind of concept is now getting popular also for small engine applications due to growing demand for low environmental impact. Well sophisticated the concept has already been for automotive

application, there are still technical issues for small engine applications, especially related to the fuel film on the wall of intake port. For example, transient behavior of the engine is emphasized much more for motorcycle application. Smaller displacement results in shorter distance between injector and the wall on the other side of the intake port. Higher engine speed is also a factor that makes design difficult.

Behavior of the fuel film generated on the intake port wall is one of the most important factors determining the air/fuel mixture distribution in PFI engine that affects the engine performance; output, exhaust emissions and transient response [1,2]. Zhao et al [3] investigated ways to reduce wall wetting in intake port and suggested that the injector type and intake port design must be adequately matched for achieving this. In order to reduce wall film, some research has focused on fuel spray and atomization using an air assisted injector. For example, Maier and Wittig [4] reported better fuel atomization than conventional injectors, which helps to reduce the wall film in the intake port and thus reduce the chances of fuel reaching the engine cylinder in the form of large droplets. The implied correlation between fuel film build-up in the intake port and HC emissions was confirmed by Felton et al [5] during their research on engine cold start.

However, generation of the wall film seems very difficult to prevent with low-pressure injection, considering the size of the generated droplets of recent injectors although it is getting smaller year by year. A reference result was reported by Nemecek et al [6], who showed that droplets with diameter less than 20 μm are easily entrained into airflow while SMD of state-of-art injectors is more than 70 μm.

Measurement techniques to quantify the property of the fuel film and its characteristics have been studied and developed by many research groups. LeCoz and Baritaud [7] introduced a quantitative method for measuring the fuel film thickness, based on the laser-induced fluorescence (LIF) technique. They found that the best tracer is 2,3-hexanedione (4% mass in iso-octane), judging by its co-evaporation similarities with the research fuel, its excitation wavelength (He-Cd laser at 441.6nm) and its fluorescence intensity. An error analysis has shown a 7% maximum error and a slightly non-linear response with film thickness up to 500 μm. Johnen and Haug [8] developed an alternative measurement system (using fiber bundle LIF) to quantify the fuel film development. They used an Ar+ cw laser tuned at 457.9nm as the light source and 5%-vol. 2,3-butanedione in iso-octane. The error in reproducibility of the determined fuel film thickness during calibration was claimed to be up to 5 μm. Lingren et al [9] developed a wall film thickness measurement device based also on LIF and suggested the measurement

accuracy to be of the order of a few microns. The light source used in their research was a pulsed Nd:YAG laser at 266nm while the fuel was iso-octane mixed 3% vol. 3-pentanone, which has similar physical properties to gasoline. Seven fibers were bundled as one centrally for transmitting the excitation light and six others were positioned coaxially for collecting the fluorescence light. Most recently, Yukihiro T. et al [10] used fiber-based LIF to measure liquid film thickness during engine cold start, where a He-Cd laser (442nm) is utilized and iso-octane is doped with 2,3-butanedione. Another technique has been reported to measure the wall film thickness without LIF by Shedd et al.[11-13]. The principle is based on the total internal reflection at the liquid surface of the light introduced from backside of the transparent wall. The size of light ring generated by the reflected light corresponds to the thickness of the film. This technique seems rather simple, although this needs transparent wall and image analysis to quantify the size of the light ring.

In this research, a fuel film thickness measurement system based on LIF has been developed, which has a rather simple setup and high accuracy. Complemented by high-speed visualization, the fuel film measurement technique in a simulated intake port has provided very interesting results about the film development; a representative sample of the results are presented here and discussed followed by conclusions.

2 EXPERIMENT APPARATUS

FUEL FILM THICKNESS MEASUREMENT SYSTEM

Various setups have been proposed for LIF-based quantitative fuel film thickness measurement [7-10] in intake ports of gasoline PFI engines; the common requirements are compatibility of the tracer with the fuel (iso-octane), sufficient fluorescence intensity of the mixture and high measurement precision and accuracy.

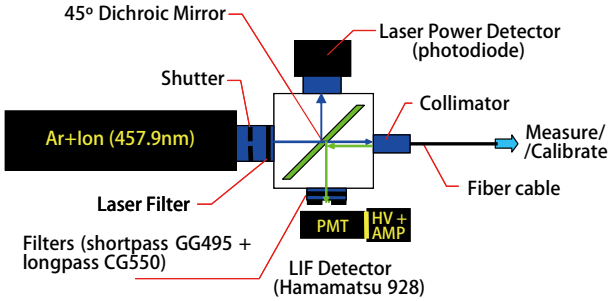

Fig.1 Schematic setup of the optical devices

Shown in **Fig.1** is the schematic setup of the optical devices. All the optical components are concentrated onto a small cubic optical box instead of being mounted on an optical bench. A fiber cable, the sensor of the system, is installed at any location on the wall measurement of the fuel film thickness. A single fiber cable is used to both transmit the excitation light and collect back the fluorescence light. The light source is an Ar+ cw laser tuned at 457.9nm. A 45° dichroic mirror is used to separate the collected fluorescence from the excitation laser light. It also reflects a small fraction of the laser light (around 2% of total power) to a photodiode as the laser power reference. Due to high sensitivity to the light intensity, a photo multiplier (PM) is used to quantify the intensity of the fluorescence. In front of the photo multiplier tube, filters are introduced to remove any unwanted light and improve the S/N ratio. In addition, a shutter is introduced to switch the passing of the laser beam for calibration purposes.

The theory behind the fuel film thickness measurement based on LIF can be described by the following equations. First, the Lambert-Beer's law shows the relationship of the incident light intensity and the light transmitted through a liquid fuel film, stated as:

$$I_{out} / I_{in} = \exp(-\alpha \cdot c \cdot \delta) \tag{1}$$

Then the intensity of the fluorescence generated within the fuel film excited by the laser is given by:

$$I_{fluor} = Q \cdot I_{in} \cdot (1 - \exp(-\alpha \cdot c \cdot \delta)) \tag{2}$$

For thin film, (2) can be approximated by the linear relationship:

$$I_{fluor} / I_{in} = Q \cdot (\alpha \cdot c \cdot \delta) \tag{3}$$

Based on this formula (3), fuel film thickness can be obtained from the laser power monitored by a photodiode and the fluorescence intensity measured by the photo multiplier, as follows:

$$\delta = k \cdot (I_{PM} / I_{PD}) \tag{4}$$

where k is determined by calibration, while the ratio inside the parenthesis is defined as the normalized LIF signal.

CALIBRATION OF FILM THICKNESS MEASUREMENT

Intensity of the LIF must be converted to fuel film thickness data using calibration data. It has been obtained by using calibration rig. An optical fiber from the same optical devices has been introduced into the rig. Fuel film thickness has been controlled using micrometer in the rig.

In this research, 5% vol. 2,3-hexanedione has been added to iso-octane as dopant. The co-evaporation characteristics of the mixture have been summarized by LeCoz and Baritaud [7]. The result of the calibration for iso-octane is shown in **Fig.2**, which indicates a linear relationship for film thickness between 0 and 200 μm. At a confidence level of 95%, the accuracy of the fuel film measurement using this in-house LIF system for iso-octane is estimated to be ± 7 μm.

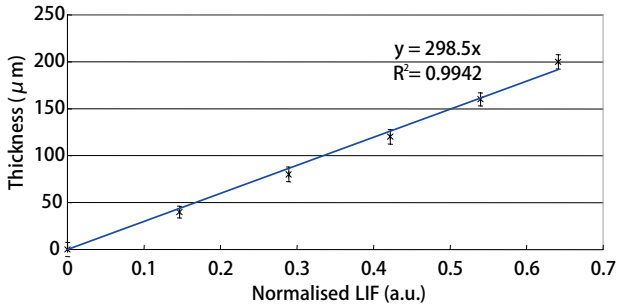

Fig.2 Calibration curve for iso-octane doped with 5% vol. 2,3-hexanedione at ambient temperature (26°C)

We have also tried to test conventional gasoline as fuel in order to know the effect of the fuel property. The calibration data for conventional gasoline without dopant has been obtained as shown in **Fig.3**. This result shows similar intensity level of the fluorescence to that with the doped iso-octane. Within the range of fuel film thickness examined in the calibration (0-200 μm), the measurement accuracy at a confidence level of 95% is also estimated to be ± 7 μm. This data has encouraged us to test also gasoline without dopant as fuel.

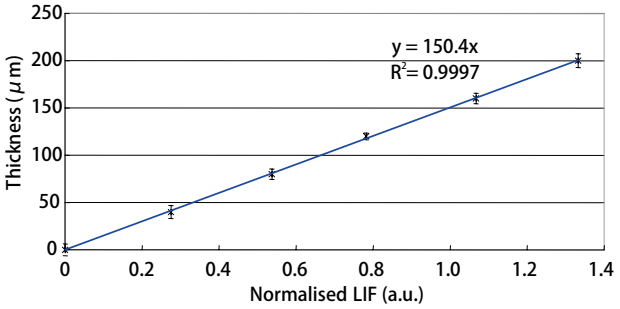

Fig.3 Calibration curve for conventional gasoline at ambient temperature (26°C)

FLOW TEST RIG

Figure 4 shows the diagram of steady flow test rig. It consists of a flow meter, an upstream dumping barrel, a throttle, and a wind tunnel called “simulated intake port”, the downstream dumping tank and a blower. The simulated intake port comprises a wind tunnel with a square section of 20mm×20mm, three transparent walls (one top and two sides) and a bottom wall whose surface is finished as cast aluminum. The wall temperature is controlled between ambient and 90°C. A fuel injector is installed on the top wall injecting fuel towards the bottom wall where the fuel film develops. The angle between injection direction and airflow is 45 degrees. The optical fiber is allowed to access the fuel film through a small hole on the wall for measuring the fuel film thickness. It is located at 50mm downstream of the injection tip location. The airflow in the simulated intake port can achieve velocity up to 100m/s and/or a depression of 0.5bar, which are representative conditions of those prevailing in an engine intake port under a typical operating regime.

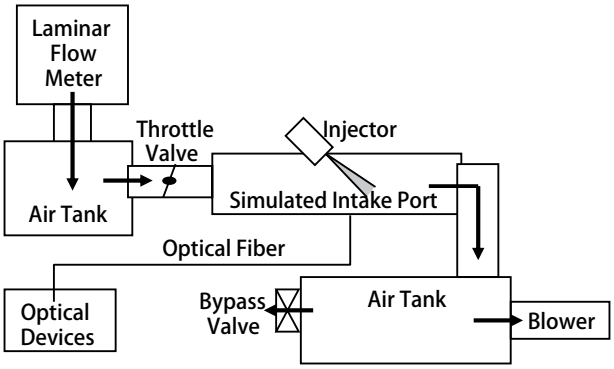

Fig.4 Diagram of Flow test rig

Figure 5 describes setup of the visualization experiments including a high-speed video to visualize the formation and development of the fuel film in the simulated intake port. The angle and location of the camera and the illuminating lamp are optimized to guarantee high quality film images. The images of the injected sprays, their impingement on the bottom wall, and wall film are captured at a sampling rate of 5000fps. Since it is impossible to apply both measurement methods at same time due to significant effect of visualization lighting to film thickness measurement, for each of the two measurement methods tests are done separately but of identical configuration.

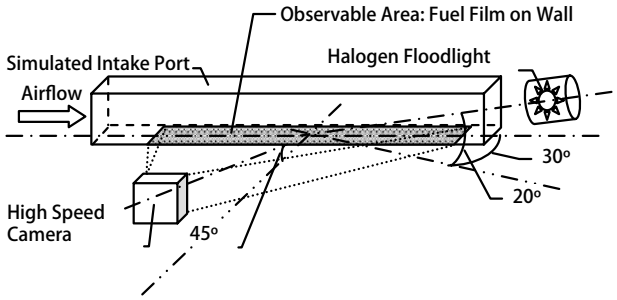

Fig.5 Setup of the visualization experiments

TEST CONDITIONS

There are a lot of parameters related with spray injection, breakup, impingement, evaporation, and film movement. **Table 1** shows a list of the parameters. The first 5 parameters in the table are variable in this report, while the others remain fixed. The reference condition is defined here as with 5ms injection duration each and 60ms injection interval, back pressure of 1bar(ambient), air velocity of 25m/s and injection pressure of 2.5bar, and the fuel of iso-octane.

Table 1. Test parameters

Fuel type	iso-octane (2,3-hexadione is doped) and gasoline
Air velocity	0, 7, 10, 15 and 25 m/s
Injection duration	3, 5, 7ms
Injection Interval	60ms (corresponding to 2000rpm)
Back pressure	0.5 and 1 bar (absolute)
Injector type	4 holes on plate
Spray angle	10 deg.
Injection pressure	2.5bar
Injection direction	45 deg. to air flow
Number of injection	11
Wall Temperature	ambient

3 RESULTS

TYPICAL DATA AND QUANTITIES OBTAINED

An example set of the images taken in this research is shown in **Fig.6**. From the first image, taken when the spray reaches the wall, gives information where and how the impingement of the spray occurs to the wall. From other images, information about the wall film can be obtained. Property of the wall film has been quantified through image processing, such as area, front and tail location, width, and so on with time-resolved manner.

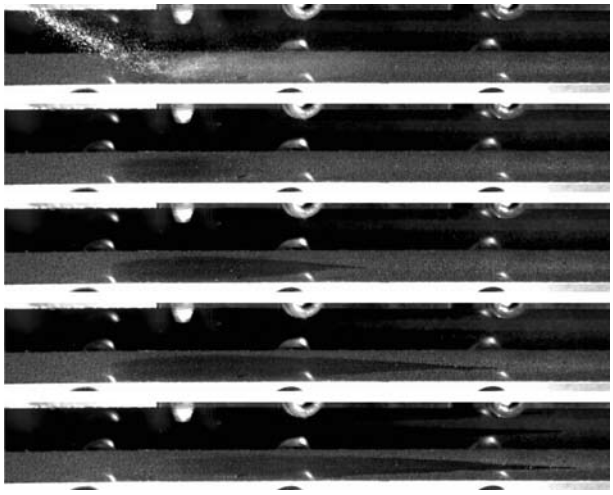

Fig.6 Spray and wall film image under reference condition
(first: impingement, second: after the first injection, third: after the 6th injection, fourth: after the 11th injection, fifth: 300ms after the 11th injection.)

Two data from the image process are used for analysis. First is initial area, which is defined as the wall film area just after the first injection. This is an index to show how large the spray impingement area is without the effect of film spreading by the airflow after stuck. Second is front speed, which is calculated from the tip front position. It is defined as the distance of the tip front position just after the first and 11^{th} (last) injection divided by the time between them. It means average velocity of the front tip of the wall film during all injections. This is an index to show how fast the film spreads on the wall. This is mainly due to the shear stress of the airflow, but includes the effect of the momentum of the spray given by impingement on the film.

Four data sets of the time-resolved film thickness are presented in **Figure 7** with the sampling rate of 1ms. Spikes with interval of 60ms correspond to injection. This data shows good repeatability of this methodology, while each data has certain level of noise. We have averaged 11 points to get better understanding from these data.

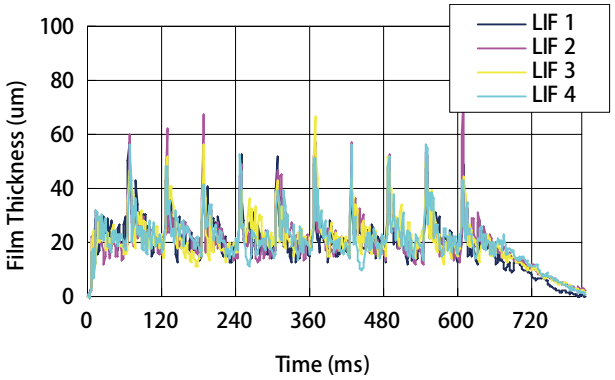

Fig.7 Wall film thickness data without average (reference condition)

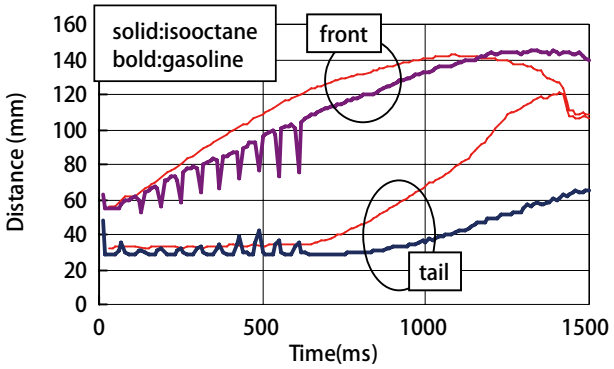

Fig.8 Effect of fuel type on wall film development (under reference condition)

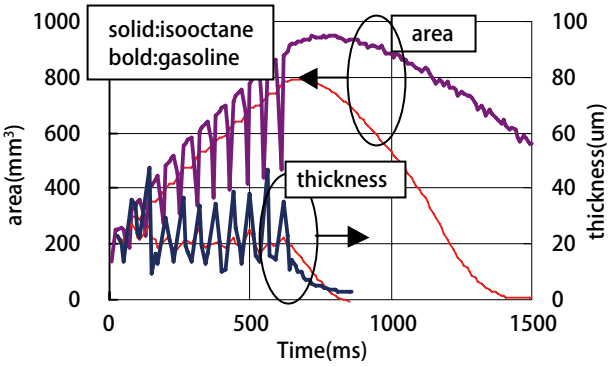

Fig.8(Cont.) Effect of fuel type on wall film development (under reference condition)

EFFECT OF FUEL TYPE

Firstly, we try to see the effect of fuel type, iso-octane and gasoline under reference condition. The results presented in **Figure 8** correspond to position of wall film front and tail, which is the distance from the injection location, and wet area and the thickness of the wall film. As shown in this figure, wall film is very similar just after the first injection. The wet area of gasoline increases more rapidly than that of iso-octane. But the front position is farther with iso-octane. This implies more rapid expansion and evaporation of the film of iso-octane than that of gasoline. This is consistent with the fact that the tail location of iso-octane moves forward soon after the all injections finish at 660ms, while that of gasoline stays until 900ms and moves forward more slowly. The average fuel film thickness of both fuels is similar, but the variation of the fuel film thickness in the case of gasoline is more significant than that for iso-octane, due to the higher volatility components of gasoline.

EFFECT OF AIRFLOW VELOCITY

Comparison of impingement patterns of the injected spray at different airflow velocity is presented on **Figure 9**. No significant change on the impingement angle is observed at low speed (0m/s and 7m/s) but a larger effect is evident at 15m/s and beyond.

Figure 10 and **Table 2** show the effect of airflow velocity on the fuel film development. The initial area also increases as the air velocity increases due to the increase of the projected impingement area on the plate. This is consistent with the images shown in **Figure 9**. The front and tail position drifts to downstream faster with increase of airflow velocity, as expected. This is consistent with the fact that the area of wall film is larger with higher airflow velocity. Let us notice that wall film area expands even under no airflow. Considering it happens mainly at the front and before injection completes, it seems that the expansion of the wall film is mainly due to the momentum of spray impingement.

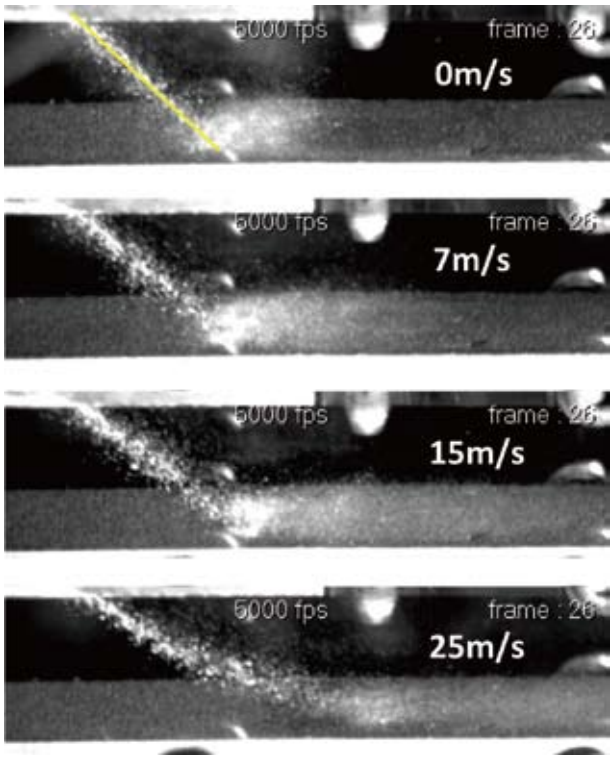

Fig.9 Effect of the airflow velocity on impingement behavior under reference condition
(first: 0m/s, second: 7m/s, third: 15m/s, fourth: 25m/s.)

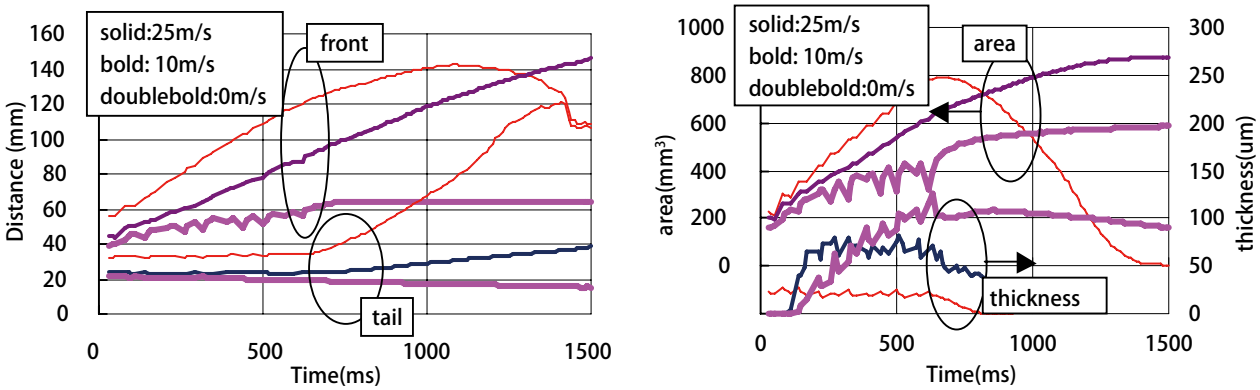

Fig.10 Effect of airflow velocity on wall film development (under reference condition except airflow)

Table 2: Effect of airflow velocity (under reference condition except airflow)

Air Velocity	0 m/s	7 m/s	10 m/s	15 m/s	25 m/s
Front speed (m/s)	0.027	0.053	0.079	0.110	0.110
Initial Area (mm^2)	152.4	192.2	207.7	222.7	245.5

The fuel film thickness starts to increase later with slower airflow. The rate of increase is also smaller with slower airflow, while the maximum of the thickness is larger. These are consistent with tendency of the film area. And the slow change of wall film thickness and area after end of injection at 660ms indicate the evaporation rate under no airflow to be very small. In other words, the evaporation of the fuel film is enhanced by the airflow very much. This effect must be taken into account when predicting the effect of the engine speed.

Judging from the front speed shown in **Table 2**, fuel film with higher air velocity lower than 25m/s spread faster. But this is not the case with 25m/s. This can be explained by considering the situation with much higher air velocity case, in which the amount of fuel stuck on the wall is little due to severer effect of the air drag force. Higher velocity also causes higher evaporation rate. Both of them are the reasons of the limitation of front speed. These effects must be taken into account when predicting the effect of the engine speed.

EFFECT OF INJECTED FUEL QUANTITY

Table 3 summarizes the effect of the fuel quantity per injection on the fuel film development. The results show that more fuel injected leads to higher film propagation speed and higher fuel film thickness as expected.

Table 3. Effect of fuel quantity (under reference condition except injection quantity)

Injection duration	3ms	5ms	7ms
Injection quantity	6.45 mm^3	10.9 mm^3	15.26mm^3
Front Speed (m/s)	0.066	0.110	0.134
Initial Area (mm^2)	196.3	245.5	234.4

More detailed information is shown in **Figure 11** about the effect of injection quantity. Interesting is the fact that the tail location and wall film thickness show very small difference, though front location moves ahead faster and area increases more rapidly with more injection quantity. This indicates the momentum given from the spray to the wall film affects severely to the development of the wall film. And it is also suggested that the increase of injection quantity does not necessarily cause accumulation of the fuel on the wall but sometimes enhances spread of the fuel film on the wall.

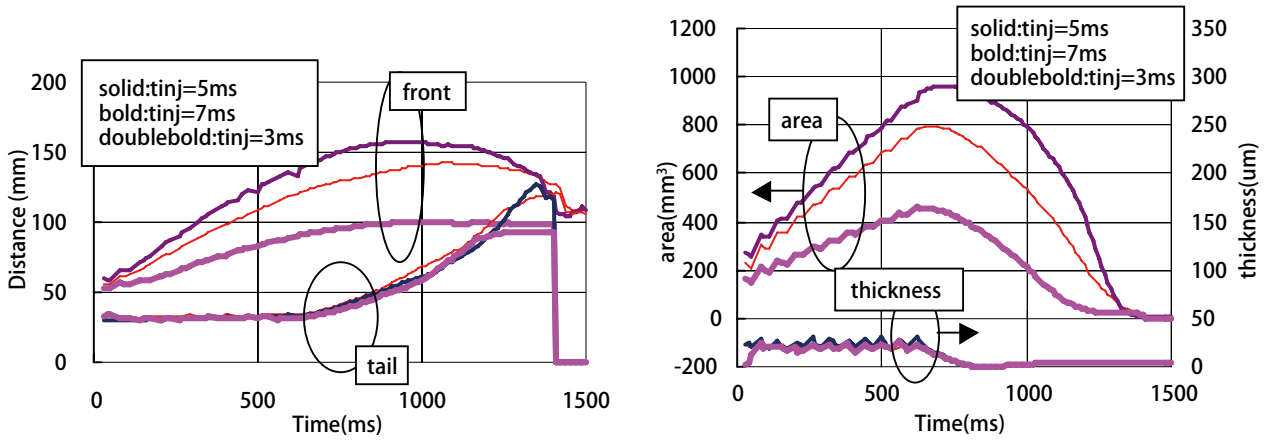

Fig.11 Effect of injection quantity on wall film development (under reference condition except quantity)

EFFECT OF INJECTION INTERVAL

Injection interval corresponds to the engine speed in the real engine operation. The effects are compared in **Figure 12**. Similar effects are expected to that of injection quantity, and almost so are they. Shorter interval of 20ms, which corresponds to 6000 rpm of 4-stroke engine, shows rapid development, but it is the matter of time scale during injections. After all 11 injections finish, wall film thickness decreases with similar speed as other cases. And the behavior of the front and tail location and film area seem to be the same as the offset of the data with the case of 60ms of injection interval. The farthest position of front and maximum of area and thickness is almost same as the case of 60ms of injection interval.

On the contrary, slower development can be seen in the case of 120ms on injection interval. The farthest position of front and maximum of area and thickness are nearer and lower than other cases. Decrease of fuel film thickness between injections can be clearly seen in this case, and the rate of decrease seems same with each other, as well as that after all injections complete. These can be summarized simply as injection interval affects almost only the time scale of the fuel film development.

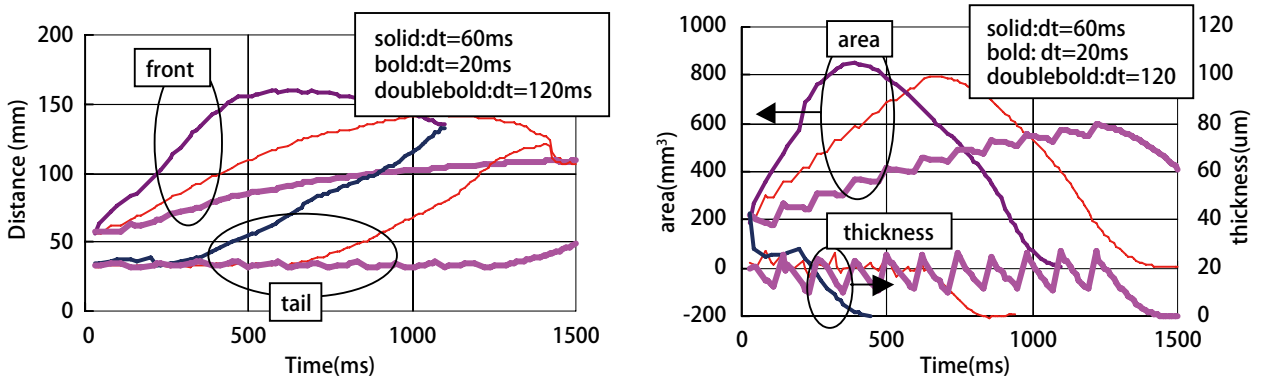

Fig.12 Effect of injection interval on wall film development (under reference condition except interval)

EFFECT OF BACK PRESSURE

Images of the spray and wall film behavior are shown in **Figure 13** under low pressure, 0.5bar. Comparing the first image with that of **Figure 6**, the location of the impingement is on the left, upstream. This indicates smaller drift of the spray by the drag force of the airflow with lower pressure. As the wall film develops, the location of the front tip and tail is similar to that of reference condition, while the width is narrower than reference condition.

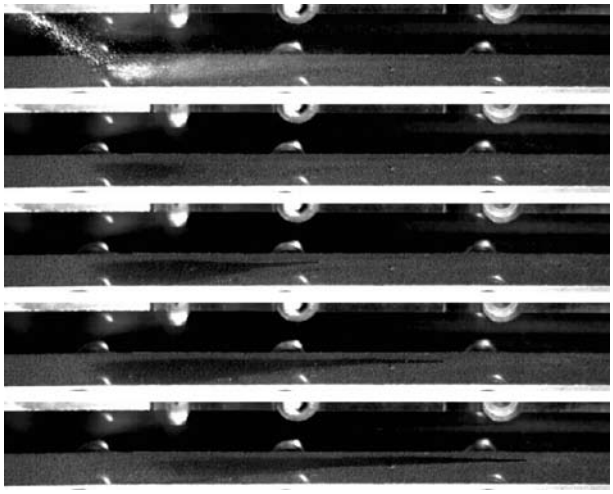

Fig.13 Behavior of the spray and wall film under low backpressure of 0.5bar (reference condition except back pressure)

The comparison in **Figure 14** and **Table 4** presents the effect of the backpressure, ambient (1bar) and 0.5bar. The front position under low pressure is behind that of ambient due to the difference of impingement location seen above. The development of the front itself shows only small difference, but the difference of area and wall film thickness is very big. The wet area under low backpressure is much lower than under ambient pressure, while the wall film is much thicker. Meanwhile, the wall film area and wall film thickness decrease rapidly after the end of injection with low-pressure condition. This results in disappearance at almost same timing of the wet area. These are caused by lower shear stress and higher evaporation rate by the airflow under low pressure. The spray impingement area is smaller under low pressure as shown in **Table 4**. These factors do not give the effect of the same direction on the development of the wall film. Lower shear stress and narrower spray angle cause slower spread of the wall film, while higher evaporation rate enhances faster decrease of the wall film. This suggests the results we have obtained by these measurements depend on the balance of these effects.

Numerical simulation may help us understand what happens in these phenomena, but we must keep in mind that the models included in the simulation, such as spray breakup and impingement, evaporation, shear stress by the airflow, and friction on the wall, are to be validated individually.

Table 4. Effect of backpressure on wall film development (under reference condition)

Back Pressure (bar)	1	0.5
Front Speed (m/s)	0.109	0.103
Initial Area (mm^2)	245.5	193

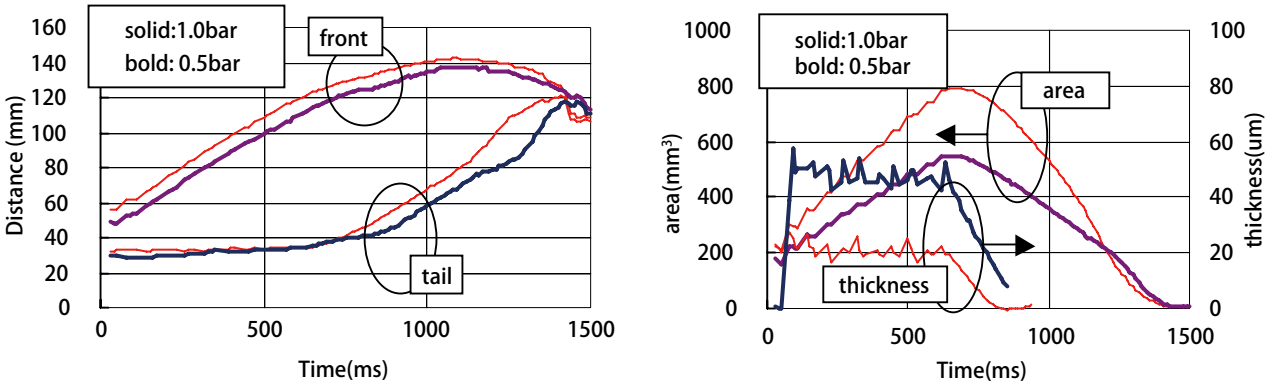

Fig.14 Effect of backpressure on wall film development (under reference condition except pressure)

4 DISCUSSION

EFFECT OF ENGINE OPERATION CONDITION

Let us consider the effect of the engine operation condition on the fuel film and mixture preparation based on the results above. Firstly, engine load relates to the injection quantity and backpressure. As the load increases, injection quantity increases and backpressure increases close to ambient. The effect of injection quantity can be predicted rather simple: increase of quantity causes more accumulation and faster spread of fuel film. The effect of backpressure is more complicated as shown above. We need think about the effect of drag force, evaporation rate, and shear stress carefully. Therefore, we cannot conclude the effect of backpressure as simple as fuel quantity. In spite of this, we can predict that higher load causes more fuel film, judging from the very big effect of injection quantity shown in **Figure 11**.

Engine speed relates to the airflow velocity, injection interval. As the engine speed increases, airflow velocity increases, while injection interval and backpressure decreases. The effect of injection interval can be predicted rather simple: decrease of interval causes more accumulation and faster spread of fuel film. Difficult is the effect of airflow velocity. Considering that the airflow velocity is nearly proportional to the engine speed, the issue of fuel film accumulation seems bigger under lower engine speed. So these effects direct inversely. Moreover, the airflow velocity changes the location of spray impingement to the wall. And the high airflow velocity also enhances the breakup of the droplet in the spray. The airflow velocity in the intake port

of small engines can reach up to 150m/s at maximum engine speed. Much bigger effect of the air to the spray is expected under such condition than seen in this experiment. Therefore, it is too difficult to conclude the effect of the engine speed within the results in this report. At least, we can say that the consideration of the interaction between the intake air and spray is very important for the design of intake system of the small engines.

5 CONCLUSION

Measurement technique for fuel film thickness, a fiber-LIF has been developed with minimum measurable fuel film thickness of 5 μm and the measurement accuracy at confidence level of 95%. Characterization of the fuel film development in a simulated intake port has been achieved through combination of fuel film thickness measurement and high-speed visualization. Investigation of the effect of various parameters on fuel film development has revealed that:

(1)Behavior of the fuel film shows difference between iso-octane and gasoline.
(2)Increase of airflow velocity causes higher propagation speed and thinner fuel film, and faster evaporation.
(3)Increase of injection quantity does not necessarily cause accumulation of the fuel on the wall but sometimes enhances spread of the fuel film on the wall.
(4)Injection interval affects almost only the time scale of the fuel film development.
(5)Lower backpressure causes smaller and thicker fuel film area in this report. It is a result of the balance of some factors, such as lower shear stress and higher evaporation rate.

Further investigations are necessary, especially on the effect of other important parameters, such as wall temperature and surface roughness.

6 ACKNOWLEDGMENTS

The authors are grateful to Dr Y. Yan in City University London for her support with the software and the processing of the acquired images.

7 NOMENCLATURE

I: Intensity of light

δ: Path length or thickness of liquid film

c: Molar concentration of tracer species

α: Absorption coefficient

Q: Quantum efficiency

k: Calibrated coefficient for film thickness measurement

Subscript

in: Incident light

out: Light passing through liquid film

fluor: Fluorescence light

PM: Measured by photo multiplier

PD: Measured by photodiode

8 REFERENCES

[1] Kato, S., Hayashida, T. and Iida, M., "The Influence of Port Fuel Injection on Combustion of a Small Displacement Engine for Motorcycle", SAE Paper 2007-32-0009.

[2] Bianchi, G.M., Brusian, F., Postrioti, L., Grimaldi, C.N., Di Palma, S., Matteucci, L., Marcacci, M. and Carmignani, L., "CFD Analysis of Injection Timing Influence on Mixture Preparation in a PFI Motorcycle engine", SAE Paper 2006-32-0022 (2006).

[3] Zhao, F.Q., Yoo, J.H. and Lai, M.C., "Spray Targeting Inside a Production-Type Intake Port of a 4-Valve Gasoline Engine", SAE Paper 960115 (1996).

[4] Maier, G., Wittig, S., and Manz, P.W., "Influence of Air Assisted Fuel Injection on the Mixing Preparation within the Intake Ports of SI-Engine", SAE Paper 982523 (1998).

[5] Felton, P.G., Kyritsis, D.C. and Fulcher, S.K., "LIF Visualization of Liquid Fuel in the Intake Manifold During Cold Start", SAE Paper 952464 (1995).

[6] Nemecek, L.M., Wagner, R.M., Drallmeier J.A., "Fuel Droplet Entrainment Studies for Minimization of Cold-Start Wall-Wetting", SAE Paper 950508 (1995).

[7] LeCoz, J.F. and Baritaud, T., "Application of Laser Induced Fluorescence for Measuring the Thickness of Liquid Films on Transparent Wall", 7th Int. Symposium of Laser Techniques to Fluid Mechanics, Lisbon (1994).

[8] Johnen, T. and Haug, M., "Spray Formation Observation and Fuel Film Development

Measurements in the Intake of a Spark Ignition Engine", SAE Paper 950511 (1995).
[9] Lindgren, R., Block R., Denbratt, I., "Development of a Wall Film Thickness Measuring Device", Inst. Phys. Conf. Ser. No. 177, 2002, pp. 83-88
[10] Yukihiro T., Yoshihiro, N. and Yuuichi, K., "Analysis of a Fuel Liquid Film Thickness on the Intake Port and Combustion Chamber of a Port Fuel Injection Engine", FISITA Paper F2006P106 (2006)
[11] T. A. Shedd and T. A. Newell, "Automated optical liquid film thickness measurement method", Review of Sci. Inst., 69(12): 4205–4213(1998).
[12] A.G. Pautsch, T.A. Shedd, "Adiabatic and diabatic measurements of the liquid film thickness," Int.J. Heat and Mass Transfer, Vol.49(15-16), 2610-2618(2006)
[13] Toshiro Kiura, Timothy A. Shedd and Benjamin C. Blaser, "Investigation of Spray Evaporation and Numerical Model Applied for Fuel-injection Small Engines", SAE Paper 2008-32-0064 (2008)

当論文は、SAE2009-32-0129・JSAE20097129として、ペナン（マレーシア）にて行われたSETC2009にて発表され、High Quality Paper ・High Quality Presentation両賞を得たものです。

■著者

飯田 実
Minoru Iida
技術本部
研究開発統括部
パワートレイン研究部

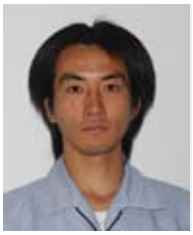

吉川 啓一
Keiichi Yoshikawa
技術本部
研究開発統括部
パワートレイン研究部